Two–Dimensional Fully Adaptive Solutions
of Reaction–Diffusion Equations

Jens Lang

Abstract

We present an adaptive Rothe method for two–dimensional problems combining an embedded Runge–Kutta scheme in time and a multi-level finite element discretization in space. The spatial discretization error is controlled by a posteriori error estimates based on interpolation techniques. A computational example for a thermodiffusive flame propagation model illustrates the high accuracy that is possible with the proposed method.

Keywords: initial boundary value problem, Rothe method, embedded Rosenbrock method, finite elements, mesh refinement.

Introduction

The permanently increasing complexity of practically relevant models requests new numerical methods to solve the underlying extensive systems of time–dependent partial differential equations. Here, adaptivity in both time and space not only leads to a drastic reducing of the computational effort, but also improves the solution in selected domains. Furthermore, the adaptive process furnishes error estimates that permit to determine the reliability of the modelling process.

Over the years, several methods of adaptive techniques have been developed. Some of them have also been applied to time–dependent systems. Bietermann and Babuška [7, 8] developed regridding methods for one–dimensional parabolic problems using finite element methods of lines procedures. Adjerid and Flaherty [1] additionally allowed to move the mesh during the temporal integration. Later they applied the method of lines to solve vector systems of parabolic partial differential equations on two–dimensional rectangular regions using bilinear finite element approximations

[2]. NOWAK [30] discussed static and dynamic regridding methods for non-linear parabolic systems in one space dimension using finite difference procedures on nonuniform meshes. The resulting software package PDEX1M is based on the efficient time–extrapolation code LIMEX which was theoretically treated by DEUFLHARD et al. [16, 17]. Another software specifically designed for the method of lines is the SPRINT package of BERZINS et al. [6]. It contains a selection of spatial discretizations, time integrators and linear algebra routines.

In contrast to the widespread method of lines there are several approaches exploiting the discretization sequence first in time then in space, well–known as classical Rothe method. So, SMOOKE [33] et al. applied an implicit Euler discretization and a two–dimensional spatial refinement that equidistributes a positive weight function over a given mesh interval in each direction at each time level. BORNEMANN established a new mathematical framework to analyze fully adaptive multilevel discretizations for scalar linear parabolic PDEs. First he treated extrapolation methods to discretize the time operator [9]. Yet structural drawbacks of these methods led to the insight that variable–order time discretizations based on a multiplicative error correction are better fit for linear time–space problems [10]. He developed further the program KASTIO including a multilevel nodal basis preconditioner to solve efficiently the linear systems arising from two–dimensional heat problems [11]. In a next step LANG and WALTER [25] presented a space–time fully adaptive method for unsteady one–dimensional reaction–diffusion systems, employing different variable–time step Runge–Kutta schemes. The resulting methods have been discussed and applied to a variety of nonlinear problems each demonstrating a different source of numerical difficulties [24]. This approach has now been extended to the two–dimensional case. For this a higher–order time scheme is utilized and the inner spatial loop is carried out with the help of the elliptic solver KASKADE [19] which is based on the multilevel ideas of DEUFLHARD et al. [15].

Let us consider the time–dependent partial differential equations of the form

$$(0.1) \quad P(x,y)\partial_t \mathbf{u} - \nabla \cdot (D(x,y)\,\nabla\,\mathbf{u}) \;=\; \mathbf{F}(x,y,t,\mathbf{u})$$

$$(x,y) \in \Omega \subset \mathbb{R}^2,\ t > 0,$$

with the initial condition

$$(0.2) \quad \mathbf{u}(x,y,0) \;=\; \mathbf{u}^0(x,y)\,, \quad (x,y) \in \Omega \cup \partial\Omega,$$

2

and the boundary conditions

$$
\begin{aligned}
(0.3) \qquad u_j(x,y,t) &= \xi_j(x,y,t)\,, \quad (x,y) \in \partial\Omega_j^D\,, \\
(0.4) \qquad \mathbf{n}^T D_{ij} \nabla u_j + \sigma_{ij}(x,y) u_j &= \zeta_{ij}(x,y,t)\,, \quad (x,y) \in \partial\Omega_j^C\,. \\
t > 0,\ i,j &= 1,\dots,m.
\end{aligned}
$$

The functions $\mathbf{u}(x,y,t)$ and $\mathbf{F}(x,y,t,\mathbf{u})$ are m–vectors, $P(x,y)$ is a $m \times m$–matrix, $D(x,y)$ is a 2×2–matrix of $m \times m$–blocks, that means

$$
D(x,y) \;=\; \begin{pmatrix} D^{11}(x,y) & D^{12}(x,y) \\ D^{21}(x,y) & D^{22}(x,y) \end{pmatrix}
$$

where $D^{kl} = (d_{ij}^{kl})_{i,j=1,\dots,m}$, $k,l = 1,2$, and $D^{12}(x,y) = D^{21}(x,y)$. Especially we set

$$
D_{ij}(x,y) \;=\; \begin{pmatrix} d_{ij}^{11}(x,y) & d_{ij}^{12}(x,y) \\ d_{ij}^{21}(x,y) & d_{ij}^{22}(x,y) \end{pmatrix}.
$$

For a shorter presentation, we use the grad– and div–operator in vector sense, namely

$$
\nabla\,\mathbf{u} = (\partial_x \mathbf{u}, \partial_y \mathbf{u})^T\,, \quad \nabla \cdot (\mathbf{u},\mathbf{v})^T = \partial_x \mathbf{u} + \partial_y \mathbf{v}\,.
$$

Furthermore, subscripts ∂_x, ∂_y, and ∂_t denote partial differentation, Ω is an open bounded polygonal domain in $\mathbb{R}^2$ with boundary $\partial\Omega = \partial\Omega_j^D \cup \partial\Omega_j^C$, $j = 1,\dots,m$, i.e. boundary conditions are prescribed for each component u_j individually and independently. The real functions ξ_j, σ_{ij} and ζ_{ij} are sufficiently smooth. Note that the Cauchy boundary conditions may be different for each equation described by the parameter i in (0.4). Finally, $\mathbf{n} = (n_1, n_2)^T$ is a unit outer normal vector to $\partial\Omega$. It is assumed here that the partial differential system (0.1)–(0.4) is of parabolic type and that it has a unique solution.

Our analysis requires the use of the L^2 inner product and norm

$$
\begin{aligned}
(0.5) \qquad (\mathbf{u},\mathbf{v}) &:= \int_\Omega \mathbf{v}^T(x,y,t)\mathbf{u}(x,y,t)\,dxdy\,, \\
\|\mathbf{v}\|_0 &:= (\mathbf{v},\mathbf{v})^{1/2}\,.
\end{aligned}
$$

Given a function v and the multi-index $\delta = (\delta_1, \delta_2)$ with $|\delta| := \delta_1 + \delta_2$, we define the usual seminorms and norms of the Sobolev spaces $H^s(\Omega)$, $s = 1,2$,

$$|\mathbf{v}|_s \quad := \quad \left(\sum_{|\delta|=s} \frac{s!}{\delta_1! \delta_2!} \|(\partial_x)^{\delta_1}(\partial_y)^{\delta_2} \mathbf{v}\|_0^2 \right)^{1/2} ,$$

$$\|\mathbf{v}\|_s \quad := \quad \left(\|\mathbf{v}\|_0^2 + \sum_{i=1}^{s} |\mathbf{v}|_i^2 \right)^{1/2} .$$

Function $\mathbf{v}$ belonging to the space $H_D^s(\Omega)$ must satisfy any Dirichlet boundary condition in (0.3), while functions in $H_0^s(\Omega)$ are further restricted to satisfy homogenous Dirichlet boundary conditions. Norms that are related to other integration domains are obtained by replacing Ω in (0.5) and adding the new domain subscript to the corresponding norm.

A large number of phenomena in chemistry, biology, and physics are governed by systems of reaction–diffusion equations. Typically, the solutions possess sharp moving spatial transitions induced by emerging boundary and internal layers, or strong reaction terms. The adaptive method described in the present paper will be useful in resolving critical regions of high spatial and temporal activity.

Our discretization sequence can be characterized as follows: first we discretize (0.1)–(0.4) in time using an efficient time integrator. There is a general understanding that only implicit methods promise good results for stiff reaction–diffusion systems. From this point of view the most prominent multistep, one–step or extrapolation methods are applicable [21]. To make an appropriate choice we have to take into account the second part of the whole discretization: find a spatial mesh at each time level well–adapted to the solution. That means, methods using a wide stencil of different time levels to construct higher order solutions, such as multistep and extrapolation methods, seem not to be favourable when the underlying spatial discretization is permanently changing. The effort of interpolation and the need of memory would quickly become too expensive. It remains the class of one–step methods that request only two different meshes: one on which the starting value is given, and a second on which the new solution is computed. Among them, linearly implicit Runge–Kutta methods have shown to give very satisfactory results for stiff equations. Their main advantage over fully–implicit methods is that nonlinear systems are completely avoided. Last but not least they are nearly as simple to implement as explicit Runge–Kutta methods.

We use a special embedded Rosenbrock method of order 3(2). Thus, the above nonlinear system is replaced by a fixed sequence of linear elliptic systems that are solved by a multilevel finite element method (FEM) with

4

linear elements. The spatial refinement process is controlled by error indicators based upon traditional interpolation techniques. They can be computed locally and are fairly inexpensive. Both components lead to temporal integration with sufficient accuracy in time and space.

The program used to manage the occuring dynamic tree data structure is a two–dimensional extension of the code KARDOS described in [26]. The underlying package KASKADE [19] permits efficient and easy access to the data when deleting or adding finite elements.

This paper is outlined as follows. In Section 1, we describe the adaptive time discretization. The space discretization and spatial error estimation follow in Section 3. Therein a special error indicator that does not penalize small angles is discussed. In Section 4, we present computational examples to illustrate the high accuracy of the proposed adaptive method.

1   Time Discretization of the Problem

We discretize (0.1)–(0.4) in time using a special linearly implicit Runge–Kutta method. For a moment we set

$$(1.1) \qquad \mathbf{f}(t, \mathbf{u}) \quad := \quad \mathbf{F}(t, \mathbf{u}) + \nabla \cdot (D\nabla \mathbf{u}) \,,$$

and get

$$(1.2) \qquad \left(\frac{1}{\tau \gamma} P - \partial_{\mathbf{u}} \mathbf{f}(0, \mathbf{u}^0) \right) \mathbf{l}^i \quad = \quad \mathbf{r}^i \,,$$

$$\mathbf{r}^i := \mathbf{f}(0 + \alpha_i \tau, \mathbf{u}^0 + \sum_{j=1}^{i-1} a_{ij} \mathbf{l}^j) + P \sum_{j=1}^{i-1} \left(\frac{c_{ij}}{\tau} \right) \mathbf{l}^j + \gamma_i \tau \partial_t \mathbf{f}(0, \mathbf{u}^0)$$

$$(1.3) \qquad l_j^i(x, y) \quad = \quad \gamma_i \left(\xi_j(x, y, \tau) - \xi_j(x, y, 0) \right) \,, \; (x, y) \in \partial \Omega_j^D \,,$$

$$\mathbf{n}^T D_{kj} \nabla l_j^i + \sigma_{kj} l_j^i \quad = \quad \gamma_i \left(\zeta_{kj}(x, y, \tau) - \zeta_{kj}(x, y, 0) \right) \,, \; (x, y) \in \partial \Omega_j^C \,,$$

$$i = 1, 2, 3, \; k, j = 1, \ldots, m \,,$$

$$(1.4) \qquad \mathbf{u}^1(\tau) \quad = \quad \mathbf{u}^0 + \sum_{j=1}^{3} b_j^1 \, \mathbf{l}^j \,,$$

$$(1.5) \qquad \mathbf{u}^2(\tau) \quad = \quad \mathbf{u}^0 + \sum_{j=1}^{3} b_j^2 \, \mathbf{l}^j \,,$$

as a 3–stage embedded Rosenbrock method with a variable time step τ. Here, the stage values $\mathbf{l}^i, i = 1, 2, 3$, are m–vectors, $\partial_{\mathbf{u}}\mathbf{f}$ is the Jacobian matrix of $\mathbf{f}$ with respect to $\mathbf{u}$. The real coefficients γ, γ_i, a_{ij}, α_i, c_{ij}, b_j^1, and b_j^2 are chosen in such a way that the solution $\mathbf{u}^1$ is of third order and $\mathbf{u}^2$ of second order, respectively. Furthermore, we request L–stability making the method stiffly accurate. The corresponding set of coefficients, see Table 2.1, was derived from a method first proposed by ROCHE [32] for differential–algebraic equations.

γ	=	0.435866521508459			
γ_1	=	0.435866521508459	α_1	=	0.0
γ_2	=	0.6044552840655588	α_2	=	0.7
γ_3	=	6.3797887993448800	α_3	=	0.7
b_1^1	=	2.236727045296589	b_1^2	=	2.059356167645941
b_2^1	=	2.250067730969645	b_2^2	=	0.169401431934653
b_3^1	=	-0.209251404439032	b_3^2	=	0.0
a_{21}	=	1.605996252195329	c_{21}	=	0.8874044410657823
a_{31}	=	1.605996252195329	c_{31}	=	23.98747971635035
a_{32}	=	0.0	c_{32}	=	5.263722371562130

Tab. 2.1: Coefficients for 3(2)–Rosenbrock time scheme

All the above features are based on the assumption that the exact Jacobian is available. This is a crucial point in the context of PDE solvers where spatial discretization errors are really present. However, the usage of an approximation of the Jacobian only, well known as W–method, leads to the computation of rather more stage values necessary to get the same accuracy as a comparable Rosenbrock method. Furthermore, high dynamics in the system under consideration or additional algebraic equations request a nearly exact Jacobian at each time step.

The embedding strategy directly supplies us with an estimator ε_t of the main error term describing the local error of the second order method,

$$(1.6) \qquad \varepsilon_t \quad := \quad \|\mathbf{u}^2 - \mathbf{u}^1\|_0 \, .$$

Given a tolerance TOL_t for the time discretization, the usual proposal for the new step size is

$$(1.7) \qquad \tau_{new} \quad := \quad \rho \left(\frac{TOL_t}{\varepsilon_t} \right)^{1/3} \tau$$

where ρ denotes a safety factor, presently set to be 0.9.

The remaining boundary value problems (1.2)–(1.3) are solved applying a multilevel FEM.

2   SPACE DISCRETIZATION OF THE PROBLEM

The starting point for the use of the FEM is the weak formulation of the corresponding boundary value problem. Assuming that $\mathbf{l}^i \in H_D^1(\Omega)$, $i = 1, 2, 3$, multiplying (1.2) by a test function $\mathbf{v} \in H_0^1(\Omega)$, and integrating it on Ω applying additionally integration by parts of the diffusion terms, we obtain

$$(2.1) \qquad B_\tau(\mathbf{l}^i, \mathbf{v}) \;\; = \;\; \mathbf{r}^i(\mathbf{v}) \qquad \text{for all } \mathbf{v} \in H_0^1(\Omega) \;,\;\; i = 1, 2, 3,$$

where

$$B_\tau(\mathbf{l}^i, \mathbf{v}) \;\; := \;\; (D\nabla \mathbf{l}^i, \nabla \mathbf{v}) + \left(\frac{1}{\tau\gamma} P\mathbf{l}^i - \mathbf{F_u}(0, \mathbf{u}^0)\mathbf{l}^i, \mathbf{v} \right) +$$

$$+ \sum_{j,k=1}^{m} \int_{\partial \Omega_j^C} \sigma_{kj} l_j^i v_k ds \;,$$

$$\mathbf{r}^i(\mathbf{v}) \;\; := \;\; (\mathbf{r}^i, \mathbf{v}) + \sum_{j,k=1}^{m} \int_{\partial \Omega_j^C} \zeta_{kj}^i v_k ds \;.$$

Selecting finite–dimensional approximations $\mathbf{L}^i \in S_D^k \subset H_D^1(\Omega)$ and $\mathbf{V} \in S_0^k \subset H_0^1(\Omega)$ of $\mathbf{l}^i$ and $\mathbf{v}$, respectively, we construct finite element solutions $\mathbf{L}^i$ of (2.1) solving the equations

$$(2.2) \qquad\qquad B_\tau(\mathbf{L}^i, \mathbf{V}) \;\; = \;\; \mathbf{r}^i(\mathbf{V}) \qquad \text{for all } \mathbf{V} \in S_0^k \;.$$

The spaces S_D^k and S_0^k consist of piecewise linear continuous polynomials over a fixed triangulation T_k. In the spirit of spatial adaptivity the solution space $H_D^1(\Omega)$ is now replaced by a sequence of discrete spaces S_D^k, $k = 0, 1, 2, \ldots$, with successively increasing dimension to improve the approximation property [15]. Clearly, new degrees of freedom should be placed only in those regions where the refinement leads to a significant reduction of the spatial error. For that, we employ the standard "red"– and "green"– refinement used e.g. in the PLTMG– and in the KASKADE–code: Selected triangles are refined into four congruent triangles ("red") and the new triangulation is made compatible by further special refinements ("green").

Once the approximate solution $\mathbf{L}^i \in S_D^k$ has been computed, a posteriori error indicators and estimators can be utilized to give specific assessment of the error distribution being a basis to form adaptive refinements. Over the years, several error estimators have been developed. Excellent surveys of adaptivity and a posteriori error estimation have appeared in [29, 31]. We turn our attention to error indicators that are based upon traditional interpolation techniques in the finite element approximation theory. Here, the work of DIAZ et al. [18] brought in some new ideas in the area of multidimensional error control. Unfortunately, they still used a very rough estimate of the interpolation error. Better estimates on quadrilateral meshes were developed by DEMKOWICZ and ODEN [13]. Our aim is to establish asymptotic interpolation errors for triangular meshes, trying not to loose any dependency of the error on the mesh geometry.

Although a priori estimated upper bounds of the approximation error can provide pessimistic indications, the corresponding error indicators are cheap and can often be quite useful to improve the grids. These indicators only require a posteriori estimation of higher–order derivatives, thus a local and fairly inexpensive computation is available.

The new approximate solutions $\mathbf{U}^i$ of $\mathbf{u}^i, i = 1, 2$, are obtained by solving three different linear systems (2.2). As experienced in the one–dimensional case, it is not necessary to include all these three problems in the spatial estimation process. According to the fact that

$$(2.3) \qquad \mathbf{u}^E \quad := \quad \mathbf{u}^0 + \frac{\mathbf{l}^1}{\gamma}$$

is exactly the semi–implicit Euler solution of (0.1), it can be assumed that a space grid well–fitted to $\mathbf{l}^1$ also works well for the solutions $\mathbf{u}^1$ and $\mathbf{u}^2$. Therefore, our aim is to construct an adaptive refinement process appropriate for the first stage value $\mathbf{l}^1$ satisfying (2.1).

To get a priori error estimates for the finite element solution $\mathbf{L}^1$, we will use the Lax–Milgram theory. For that, the following assumptions are made: There exist constants $c_i^P > 0, c_i^H > 0, i = 0, 1$, and $\lambda^H \geq 0$ such that

$$
\begin{aligned}
|(P\mathbf{v}, \mathbf{w})| &\leq c_0^P \, \|\mathbf{v}\|_0 \, \|\mathbf{w}\|_0 \,, \\
|(H\mathbf{v}, \mathbf{w})| &\leq c_0^H \, \|\mathbf{v}\|_1 \, \|\mathbf{w}\|_1 \,, \quad \mathbf{v}, \mathbf{w} \in H^1(\Omega) \,, \\
(P\mathbf{v}, \mathbf{v}) &\geq c_1^P \, \|\mathbf{v}\|_0^2 \,, \\
(H\mathbf{v}, \mathbf{v}) &\geq c_1^H \, \|\mathbf{v}\|_1^2 - \lambda^H \|\mathbf{v}\|_0^2 \,, \quad \mathbf{v} \in H_D^1(\Omega) \,,
\end{aligned}
$$

(2.4)

with

$$Hv := -\nabla \cdot (D\nabla v) - \partial_u F(0, u^0)v .$$

Here, the operators P and H are imposed with the corresponding boundary conditions and should be understood in the weak sense. All assumptions are quite general in the context of linear elliptic operators, see for instance [12]. Especially, the last inequality is related to the fact that the strict positivity of the operator H is in general disturbed by large positive eigenvalues of the Jacobian matrix F_u describing time-dependent growth of some solution components. These dynamics request sufficiently small time steps to ensure existence and uniqueness of the solutions l^i in (1.2). Therefore, we further assume

$$(2.5) \qquad \frac{c_1^P}{\gamma} - \tau\lambda^H \geq c^H > 0 .$$

This condition is similar to those we have got from analyzing time discretizations derived from Newton's method [24].

Defining the τ–dependent norm

$$(2.6) \qquad \|v\|_{1,\tau}^2 := \frac{1}{\tau}\|v\|_0^2 + \|v\|_1^2 , \quad v \in H^1(\Omega) , \ \tau > 0 ,$$

we are now able to establish the H_D^1–ellipticity of the bilinear form $B_\tau(\cdot, \cdot)$ with respect to this norm.

LEMMA 1. *With all assumptions (2.4) and (2.5) fulfilled, we have*

$$|B_\tau(v, w)| \leq c_0\|v\|_{1,\tau}\|w\|_{1,\tau} \quad \text{for all } v, w \in H^1(\Omega) ,$$

and

$$B_\tau(v, v) \geq c_1\|v\|_{1,\tau}^2 \quad \text{for all } v \in H_D^1(\Omega) ,$$

with constants $c_0 > 0$ and $c_1 > 0$ independent of τ.

Proof: Applying the Cauchy–Schwartz inequality, setting $c_0 := \max\{c_0^P/\gamma, c_0^H\}$ and $c_1 := \min\{c^H, c_1^H\}$, we get

$$
\begin{aligned}
|B_\tau(v, w)| &= \left|\left(\left(\frac{1}{\gamma\tau}P + H\right)v, w\right)\right| \\
&\leq \frac{1}{\gamma\tau}c_0^P\|v\|_0\|w\|_0 + c_0^H\|v\|_1\|w\|_1 \\
&\leq c_0\left(\frac{1}{\tau}\|v\|_0^2 + \|v\|_1^2\right)^{1/2}\left(\frac{1}{\tau}\|w\|_0^2 + \|w\|_1^2\right)^{1/2} .
\end{aligned}
$$

Furthermore,

$$
\begin{aligned}
B_\tau(\mathbf{v}, \mathbf{v}) &= \left(\left(\frac{1}{\gamma\tau} P + H \right) \mathbf{v}, \mathbf{v} \right) \geq \frac{c_1^P}{\gamma\tau} \|\mathbf{v}\|_0^2 + c_1^H \|\mathbf{v}\|_1^2 - \lambda^H \|\mathbf{v}\|_0^2 \\
&\geq \frac{c^H}{\tau} \|\mathbf{v}\|_0^2 + c_1^H \|\mathbf{v}\|_1^2 \geq c_1 \left(\frac{1}{\tau} \|\mathbf{v}\|_0^2 + \|\mathbf{v}\|_1^2 \right) . \qquad \square
\end{aligned}
$$

In direct consequence of the relations $S_D^k \subset H_D^1 \subset H^1$ and $S^k \subset H^1$, the above lemma holds also for the finite element subspace pair (S^k, S_D^k).

LEMMA 2. *With all assumptions (2.4) and (2.5) fulfilled, we have*

$$
|B_\tau(\mathbf{V}, \mathbf{W})| \leq c_0 \|\mathbf{V}\|_{1,\tau} \|\mathbf{W}\|_{1,\tau} \quad \text{for all } \mathbf{V}, \mathbf{W} \in S^k ,
$$

and

$$
B_\tau(\mathbf{V}, \mathbf{V}) \geq c_1 \|\mathbf{V}\|_{1,\tau}^2 \quad \text{for all } \mathbf{V} \in S_D^k ,
$$

with constants $c_0 > 0$ and $c_1 > 0$ independent of τ and the triangulation T_k.

As a first result in the direction of abstract error estimates, we can now apply Cea's lemma: There exists a constant C independent of the subspace S^k (and τ) such that

$$
(2.7) \qquad \|\mathbf{l}^1 - \mathbf{L}^1\|_{1,\tau} \leq C \inf_{\mathbf{V} \in S_D^k} \|\mathbf{l}^1 - \mathbf{V}\|_{1,\tau} .
$$

The constant C can be specified by the quotient c_0/c_1. The inequality (2.7) describes the quasi–optimality of the finite element approximation $\mathbf{L}^1$ with respect to the τ–norm.

The next step is to estimate the distance of the right–hand side of (2.7) by means of the Lagrangian interpolant $\mathcal{L}_k \mathbf{l}^1$ of the solution $\mathbf{l}^1$. The interpolation process is carried out componentwise on the triangulation T_k such that $\mathcal{L}_k \mathbf{l}^1(x_i, y_i) = \mathbf{l}^1(x_i, y_i)$ for all nodes (x_i, y_i). This gives the inequality

$$
(2.8) \qquad \|\mathbf{l}^1 - \mathbf{L}^1\|_{1,\tau} \leq C \|\mathbf{l}^1 - \mathcal{L}_k \mathbf{l}^1\|_{1,\tau} .
$$

Here, we have to ensure that the solution $\mathbf{l}^1$ is smooth enough in order that its Lagrangian interpolant is well defined. According to Sobolev's embedding lemma, H^2–regularity of $\mathbf{l}^1$ is supported in the following.

10

The polygonal domain $\bar{\Omega}$ can be written as a union of all triangles T that belong to the triangulation T_k. Defining $\mathcal{L}_T \mathbf{l}^1 := (\mathcal{L}_k \mathbf{l}^1)|_T$, we can split up the norm in (2.8) and get

$$(2.9) \qquad \|\mathbf{l}^1 - \mathbf{L}^1\|_{1,\tau} \;\leq\; C \left(\sum_{T \in T_k} \|\mathbf{l}^1 - \mathcal{L}_T \mathbf{l}^1\|_{1,\tau,T}^2 \right)^{1/2} .$$

Consequently, the problem of finding an a priori error estimate of the finite element solution $\mathbf{L}^1$ is reduced to the problem of estimating the local interpolation error on the triangulation T_k. This is the object of the following section.

2.1 LOCAL INTERPOLATION ERROR BOUNDS

General error bounds of local interpolation processes have been studied intensively, and are nowadays standard for the finite element theory. Nevertheless it is worthwhile to have a closer look at the assumptions obviously being made. To derive uniform estimates some regularity of the triangulation is often requested. It requires the quotient of the diameter and the inner circle radius of the triangle to be bounded, or the well–known minimal angle condition to be satisfied. These assumptions are not useful for adaptive mesh refinement, where often small and long elements are needed. SYNGE [34] was probably the first who suggested that it is better to pay attention to angles that tend to π rather than to those that tend to zero. There are several later approaches connected with this problem [3], [23].
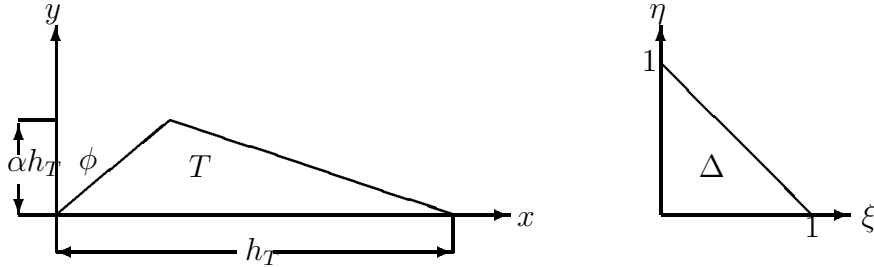

Fig. 2.1: Triangles T and Δ

Here, we want to use only the maximum angle condition, that means

$$\varrho(T) \leq \varrho_0 < \pi , \qquad \text{for all } T \in T_k ,$$

11

where $\varrho(T)$ denotes the maximum angle of T. According to the componentwise applied interpolation process, we can restrict ourselves to scalar functions v within this section.

Since the norms of $H^s(\Omega)$ are invariant with respect to the rotation of the coordinates, we can consider the case when one side of the triangle $T \in T_k$ is along a coordinate axis (see Fig. 2.1).

Without loss of generality, we set $0 < \alpha \leq 1$ and $|\phi| < \pi/2$. Further, let $\lambda := \tan\phi$. Denoting by Δ the unit triangle with the vertices $P_1 = (0,0)$, $P_2 = (1,0)$ and $P_3 = (0,1)$ the affin–linear mapping $F : \Delta \to T$ is provided by

$$
(2.10) \qquad
\begin{aligned}
x &= h_T\,\xi + \alpha\,\lambda\,h_T\,\eta\,, \\
y &= \alpha\,h_T\,\eta\,, \qquad (\xi,\eta) \in \Delta\,.
\end{aligned}
$$

For the Jacobian matrix J of this mapping, the determinant is $|J| = \alpha h_T^2$. The inverse mapping $F^{-1} : T \to \Delta$ is given by

$$
(2.11) \qquad
\begin{aligned}
\xi &= \frac{1}{h_T}x - \frac{\lambda}{h_T}y\,, \\[2mm]
\eta &= \frac{1}{\alpha h_T}y\,, \qquad (x,y) \in T\,.
\end{aligned}
$$

Next we define the space

$$
\mathcal{E}_\Theta := \{v \in H^2(\Theta) : \ v(x,y) = 0 \text{ in the vertices of } \Theta\}\,,
$$

which is employed with $\Theta = T$ and $\Theta = \Delta$. The results of the following Lemmas will be used in the subsequent proof.

LEMMA 3. (Babuška & Aziz [3])
For $v \in \mathcal{E}_\Delta$ let

$$
I_1(\alpha) := \int_\Delta \left[\left(\frac{\partial v}{\partial \xi}\right)^2 + \alpha^{-2}\left(\frac{\partial v}{\partial \eta}\right)^2 \right]\,d\xi d\eta
$$

and

$$
I_2(\alpha) := \int_\Delta \left[\left(\frac{\partial^2 v}{\partial \xi^2}\right)^2 + 2\alpha^{-2}\left(\frac{\partial^2 v}{\partial \xi \partial \eta}\right)^2 + \alpha^{-4}\left(\frac{\partial^2 v}{\partial \eta^2}\right)^2 \right]\,d\xi d\eta\,.
$$

Then there exist $A^2 > 0$, such that for all α with $0 < \alpha \leq 1$

$$A^2 \leq \inf_{v \in \mathcal{E}_\Delta} \frac{I_2(\alpha)}{I_1(\alpha)} \ .$$

LEMMA 4. (Weiss, in [28])
Let $v \in \mathcal{E}_\Delta$. Then

$$\|\mathbf{v}\|_{1,\Delta}^2 \leq 0.2587 \ |\mathbf{v}|_{2,\Delta}^2 \ .$$

We note that the constant $c = 0.2587$ was computed as the smallest positive eigenvalue μ of the eigenvalue problem

$$M(v, w) = \mu N(v, w) \ , \quad v, w \in \mathcal{E}_\Delta \setminus \{0\} \ ,$$

where M and N are the corresponding bilinear forms for the seminorm $|\cdot|_{2,\Delta}^2$ and the norm $\|\cdot\|_{1,\Delta}^2$, respectively.
We now formulate the main result of this section.

LEMMA 5. *Let $v \in \mathcal{E}_T$. Then*

$$(2.12) \qquad \|v\|_{0,T}^2 \ \leq \ 0.2587 \, (1 + |\lambda| + \lambda^2)^2 \, h_T^4 \, |v|_{2,T}^2$$

and

$$(2.13) \qquad |v|_{1,T}^2 \ \leq \ A^{-2} \, (1 + |\lambda| + \lambda^2)^3 \, h_T^2 \, |v|_{2,T}^2 \ .$$

Proof: To prove this lemma we shall employ the standard technique using the transformation of $T \in T_k$ into Δ. However, all estimates will be done with sufficient care to ensure that reliable computational error estimates can be derived. Transforming the integrals over T to Δ by means of (2.10), we obtain with

$$\hat{v}(\xi, \eta) := v(x(\xi, \eta), y(\xi, \eta)) \ \in \mathcal{E}_T$$

for all α with $0 < \alpha \leq 1$

$$(2.14) \qquad \|v\|_{0,T}^2 \ = \ \int_\Delta |\hat{v}(\xi, \eta)|^2 \, |J| d\xi d\eta = \alpha h_T^2 |\hat{v}|_{0,\Delta}^2$$

13

and

$$|v|_{1,T}^2 \;=\; \int_\Delta |J^{-T}\nabla\hat{v}(\xi,\eta)|^2 \, |J| d\xi d\eta$$

$$(2.15) \qquad \leq\; \alpha \int_\Delta \left[(1+|\lambda|+\lambda^2)\left(\frac{\partial\hat{v}}{\partial\xi}\right)^2 + \alpha^{-2}(1+|\lambda|)\left(\frac{\partial\hat{v}}{\partial\eta}\right)^2 \right] d\xi d\eta$$

$$\leq\; \alpha\,(1+|\lambda|+\lambda^2)\int_\Delta \left[\left(\frac{\partial\hat{v}}{\partial\xi}\right)^2 + \alpha^{-2}\left(\frac{\partial\hat{v}}{\partial\eta}\right)^2 \right] d\xi d\eta\;.$$

According to Lemma 4 and 3, we immediately get in (2.14)

$$(2.16) \qquad \|v\|_{0,T}^2 \;\leq\; \alpha h_T^2 \|\hat{v}\|_{1,\Delta}^2$$

$$\leq\; 0.2587\,\alpha\,h_T^2\,|\hat{v}|_{2,T}^2 \leq 0.2587\,\alpha\,h_T^2\,I_2(\alpha)\;.$$

Due to Lemma 3 there exists $A^2 > 0$ such that in (2.15)

$$(2.17) \qquad |v|_{1,T}^2 \;\leq\; \alpha\,(1+|\lambda|+\lambda^2)\,A^{-2}I_2(\alpha)\;.$$

It remains transformation of $I_2(\alpha)$ back to the triangle T. We have by (2.11)

$$I_2(\alpha) \;=\; \int_\Delta \left[\left(\frac{\partial^2\hat{v}}{\partial\xi^2}\right)^2 + 2\alpha^{-2}\left(\frac{\partial^2\hat{v}}{\partial\xi\partial\eta}\right)^2 + \alpha^{-4}\left(\frac{\partial^2\hat{v}}{\partial\eta^2}\right)^2 \right] d\xi d\eta$$

$$=\; h_T^4 \int_T \left[\left(\frac{\partial^2 v}{\partial x^2}\right)^2 + 2\alpha^{-2}\left(\alpha\lambda\frac{\partial^2 v}{\partial x^2} + \alpha\frac{\partial^2 v}{\partial x\partial y}\right)^2 + \right.$$

$$\left. + \alpha^{-4}\left(\alpha^2\lambda^2\frac{\partial^2 v}{\partial x^2} + 2\alpha^2\lambda\frac{\partial^2 v}{\partial x\partial y} + \alpha^2\frac{\partial^2 v}{\partial y^2}\right)^2 \right] |J^{-1}| dx dy\;.$$

Squaring the three expressions and applying the inequality $2ab \leq a^2 + b^2$ to the mixed terms, we easily find that

$$(2.18) \qquad I_2(\alpha) \;\leq\; (1+|\lambda|+\lambda^2)^2\alpha^{-1}h_T^2|v|_{2,T}^2\;.$$

Combining the inequalities (2.17) and (2.16) we arrive at the lemma. $\quad\square$

The unknown constant A^2 in Lemma 3 was specified in [3] as

$$A^2 \;=\; \inf_{v\in\Theta} \frac{|v|_{1,\Delta}^2}{\|v\|_{0,\Delta}^2}\;,$$

with $\Theta := \{v \in H^1(\Delta) : \int_0^1 v(0,\eta)d\eta = 0\}/\{0\}$. For practical computation one can estimate A^2 in the following way

$$A^2 \geq \inf_{v \in \tilde{\Theta}} \frac{|v|_{1,\Delta}^2}{\|v\|_{0,\Delta}^2} = \pi^2,$$

$\tilde{\Theta} = \{v \in H^1(\Delta) : v \neq \text{const.}\}$. The inequality is a direct consequence of $\Theta \subset \tilde{\Theta}$. The minimization of the new Rayleigh quotient is equivalent to seeking for the minimal positive eigenvalue of the Neumann problem for the Laplacian on the standard triangle Δ [22].

An immediate consequence of Lemma 5 is the inequality

$$(2.19) \qquad \|\mathbf{l}^1 - \mathcal{L}_T \mathbf{l}^1\|_{1,\tau,T}^2 \leq C(\tau,\lambda)|\mathbf{l}^1|_{2,T}^2$$

where

$$C(\tau,\lambda) = \left(1 + |\lambda| + \lambda^2\right)^2 h_T^2 \left(0.2587 \left(1 + \frac{1}{\tau}\right) h_T^2 + \frac{1}{\pi^2}\left(1 + |\lambda| + \lambda^2\right)\right)$$

for all $T \in T_k$. The constant $C(\tau,\lambda)$ is an increasing function of the maximum angle $\varrho(T)$, but independent of the minimum angle of the triangle T.

2.2 Control of the Spatial Error

As the mesh only consists of linear elements, the seminorm $|\mathbf{L}^1|_{2,T}$ vanishes for each element T, independent of the solution. This is remedied by extending the elements slightly beyond its boundary and integrating the second derivatives of the linear function $\mathbf{L}^1$ in the sense of distributions. Then the local H^2 seminorm of $\mathbf{L}^1$ is related to gradient jumps across the boundaries of the element. In this way we obtain the approximation

$$(2.20) \qquad |\mathbf{l}^1|_{2,T}^2 \sim D_T^2 \mathbf{L}^1 := \text{meas}(T)\frac{1}{2}\sum_{\delta \in \partial T}\sum_{i=1}^{m}\left(\left|\left[\nabla L_i^1\right]_\delta\right|/h_\delta\right)^2,$$

where $[\cdot]_\delta$ is the jump across the edge δ of T being of length h_δ. The factor $1/2$ comes from distributing the jump across ∂T over the two finite elements interfacing at ∂T. A similar operator was proposed in [20]. Of course, more sophisticated techniques are available [14]. One advantage of the suggested technique is that it is suited for arbitrary irregular meshes and that its computational effort is very low.

Summarizing all the above inequalities and the approximation (2.20) we end up with the a posteriori error estimate

$$(2.21) \qquad \|\mathbf{l}^1 - \mathbf{L}^1\|_{1,\tau} \ \leq \ C \left(\sum_{T \in T_k} \eta_T^2 \right)^{1/2} ,$$

$$\eta_T^2 \ := \ C^2(\tau, \lambda) \, D_T^2 \mathbf{L}^1 .$$

The error indicator η_T may be viewed as an asymptotical upper bound for the norm of the error on $T \in T_k$. In order to produce a nearly optimal mesh, triangles with a large error should be refined. This technique usually equilibrates the local errors on the whole mesh in several iterations and improves locally the finite element solution.
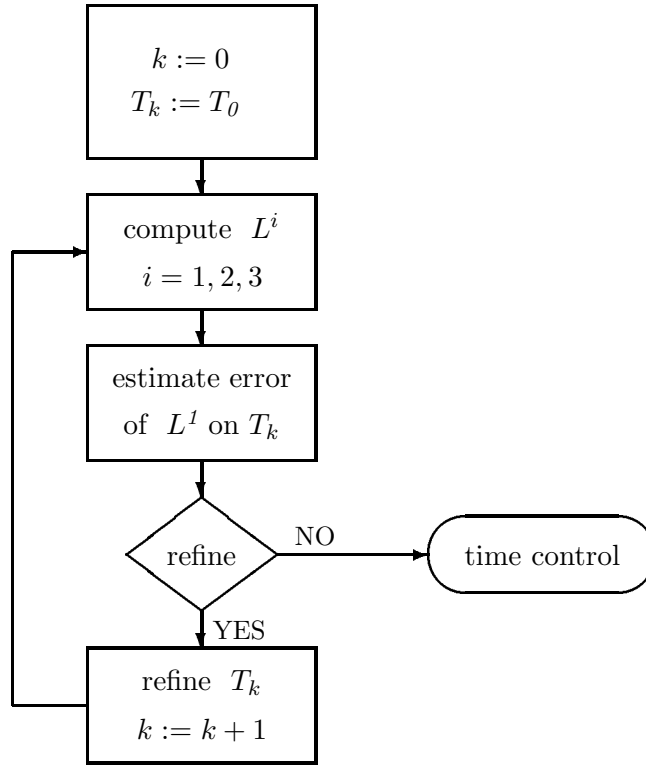
Fig. 2.2: Flow diagram for a multilevel iterative solver

Implementing the adaptive mesh algorithm we first solve the boundary value problem for $\mathbf{l}^1$ on a coarse mesh T_0. Then the average value of all the error

indicators η_T is obtained and all triangles having a greater indicator are refined. The procedure is continued until a desired local tolerance is reached. Once the refined grid is formed, we solve the linear systems with the BI–CGStab algorithm preconditioned by a SSOR method. Its convergence behaviour is very smooth and in most of the cases it converges considerably faster than other methods.

In order to get good starting values for the multilevel iteration process of the values $\mathbf{l}^2$ and $\mathbf{l}^3$ all stage problems are solved on each refinement level. In Figure 2.2 the flow diagram for the whole adaptive iteration approach is pictured.

3   NUMERICAL EXAMPLES

Example 1: To demonstrate the reliability of the proposed spatial error estimator, we consider the linear problem

$$
\begin{aligned}
-\Delta u + u &= f(x,y)\,, & (x,y) \in \Omega = \{(x,y)|\, 0 < x, y < 1\}, \\
u(x,y) &= \xi(x,y)\,, & (x,y) \in \partial\Omega,
\end{aligned}
\tag{3.1}
$$

where the functions $f(x,y)$ and $\xi(x,y)$ are such that the exact solution of (3.1) is

$$
u(x,y) = \frac{1}{2}\left[1 - tanh(20x + 16y - 4)\right].
$$

This solution exhibits a sharp transition between the nearly uniform states – a typical situation for reaction–diffusion problems. We solved (3.1) with our adaptive multilevel finite element method using the error indicator η_T for $\tau \to \infty$.

N	$\|u - U\|_1$	Ξ
274	9.633e-3	0.14
787	8.228e-3	0.23
2459	4.535e-3	0.24
7706	2.652e-3	0.24

Tab. 4.1: Number of degrees of freedom, discretization error, and effectivity index for adaptive solution of (3.1)

The resulting H^1-errors $\|u - U\|_1$ and the effectivity index

$$\Xi := \|u - U\|_1 / \left(\sum_T \eta_T^2 \right)^{1/2}$$

with respect to the degrees of freedom N are presented in Table 4.1. The convergence behaviour of the effectivity index indicates that the approximate error is indeed an upper bound of the discretization error. The important thing here is that the underlying inequalities and approximations lead to a nearly uniform overestimation of the spatial error. Accepting this fundamental fact of interpolation error estimates we can use the proposed spatial control mechanism to improve considerably the spatial discretization in the course of temporal integration.

Example 2: We are now interested in the numerical simulation of a two–dimensional premixed flame propagating in gaseous mixture. Some simplifications of the underlying physical processes lead to the so–called thermodiffusive model described by the reaction–diffusion equations

$$(3.2) \qquad \partial_t T - \triangle T = R(T, Y) + V \partial_x T ,$$

$$\partial_t Y - \frac{1}{Le} \triangle Y = -R(T, Y) + V \partial_x Y ,$$

where T is a normalized temperature variable, Y is the reduced mass fraction of the reactant, and the Lewis number Le is the ratio of thermal and species diffusion coefficient. We will use a normalized reaction rate given by

$$R(T, Y) = \frac{\beta^2}{2 \, Le} Y \, exp \left[\frac{-\beta(1 - T)}{1 - \alpha(1 - T)} \right] .$$

Here β denotes the reduced activation energy and α is the positive heat release parameter. The computational domain is a finite rectangular channel $\Omega = \{(x, y) : -8 < y < 8, \ 0 < x < 60\}$. The initial data is chosen to represent a planar steady flame in the limit $\beta \to \infty$:

$$T^0 = \begin{cases} \exp(x - x_0) & \text{for } x \leq x_0 , \\ 1.0 & \text{otherwise} , \end{cases}$$

$$Y^0 = \begin{cases} 1.0 - \exp(Le \ (x - x_0)) & \text{for } x \leq x_0 , \\ 0.0 & \text{otherwise} . \end{cases}$$

Furthermore, homogenous Neumann conditions are imposed at the whole tube wall except a special part. This part is $A = \{(x, y) \in \partial\Omega : (y = $

8) or $(y = -8)$, $30 \leq x \leq 37.5\}$, where the temperature is forced to be equal to the adiabatic flame temperature $T_A = 1$. This additional condition represents a thermally anchoring of the flame and inhibits its propagation through the reactor. The convection terms VT_x and VY_x on the right–hand side of the equations (3.2) are due to the inflow of fresh mixture at the left end of the channel. The problem is solved for the parameters $Le = 1$, $\beta = 10$, $\alpha = 0.84$, $V = -5$, and $x_0 = 28$.
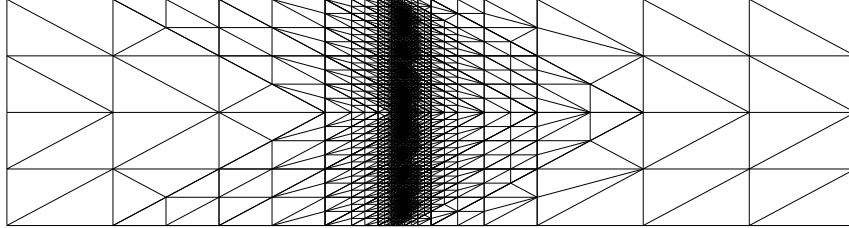

Fig. 4.1: Adaptive grid at t=0.0, 2100 nodes
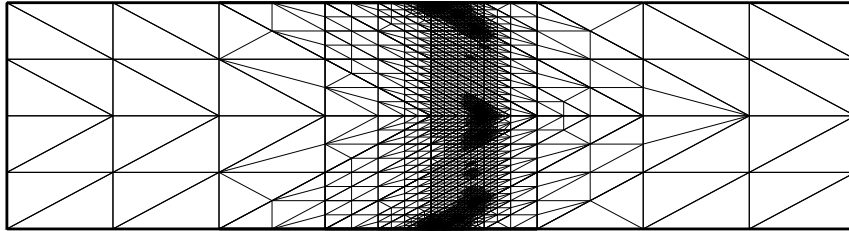
Fig. 4.2: Adaptive grid at t=1.35, 2900 nodes
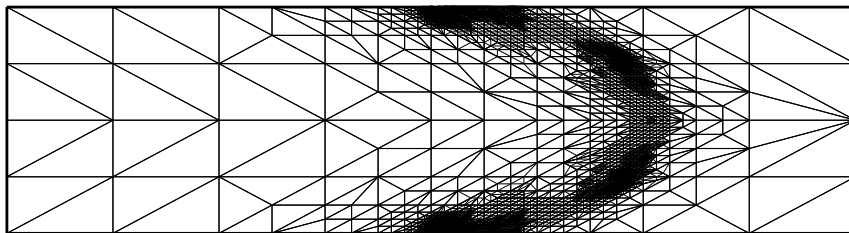
Fig. 4.3: Adaptive grid at t=4.29, 14000 nodes

A simulation of the flame propagation requires a dense computational mesh in the thin flame region, and especially in the boundary layer caused by the time–fixed Dirichlet condition. The computation at each time level starts

with a uniform coarse mesh of 64 triangles. First experiences have shown that at least a time tolerance $TOL_t = 1.0e - 4$ is needed to reflect exactly the temporal dynamic. The spatial local tolerance is set to be 0.2 with respect to the above introduced τ–norm. This tolerance forces the usage of 2000 nodes at the beginning and of 14000 nodes at the end, which means about 30000 unknowns with respect to a refinement depth of 13 levels. Note, that about 10^{10} triangles would be needed to guarantee the same accuracy on a uniform mesh.
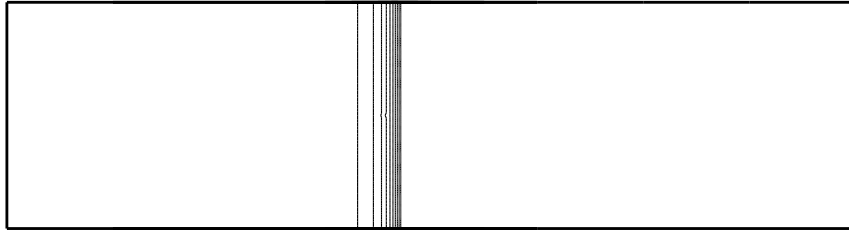

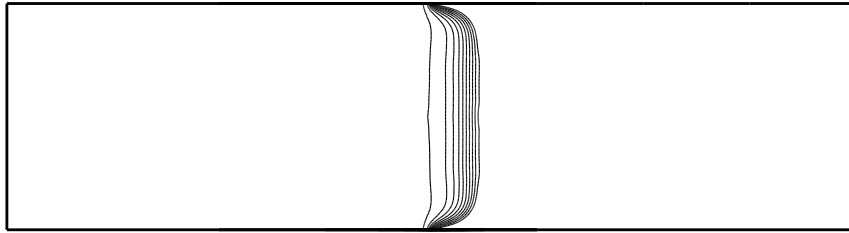Fig. 4.4: Adaptive solution at t=0.0

Fig. 4.5: Adaptive solution at t=1.35

Fig. 4.6: Adaptive solution at t=4.29

The corresponding finite element triangulations are shown in Fig. 4.1–4.3. Two special cuts through the computational domain show the high resolution of the proposed scheme within the steep flame front.
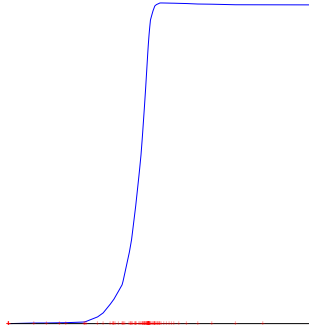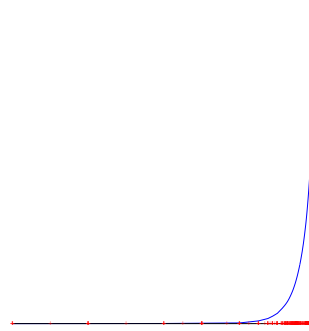
Fig. 4.7: Cut 1 from
(30.0,0.0) to (60.0,0.0)

Fig. 4.8: Cut 2 from
(31.0,0.0) to (31.0,8.0)

4 CONCLUSION

We developed a third order Runge–Kutta scheme and a multilevel linear
finite element approximation to calculate the solutions of parabolic partial
differential equations. Selfadaptive mesh refinement based on local interpola-
tion error estimates and time step control using an embedded strategy seem
to be suitable for an automatic solution of nonlinear problems governed by
the reaction–diffusion mechanism. The results of the example provide an
indication of the high resolution of the proposed method. This difficult non-
linear problem was solved without any a priori knowledge of the solution, no
special initial mesh was used.

Nevertheless, there is a great interest to improve the performance of our
spatial refinement process. Methods for elliptic problems [4, 5] that utilize
local auxiliary problems to compute error estimates should also be used for
two–dimensional parabolic systems. The relationship between spatial and
temporal accuracy in an adaptive approach is a further important area when
seeking software with high reliability. LAWSON et al. [27] presented a ba-
lancing strategy in the method of lines approach. For the Rothe method,
BORNEMANN [10] and later LANG and WALTER [24] advocate matching the
spatial errors in such a way that a prescribed global tolerance is achieved.
In addition, we plan to include anisotropic refinement strategies to enhance
further the resolution of the solutions.

5 Acknowledgement

I would like to thank R. Roitzsch for his permanent support to solve tricky programming problems, and Dr. J. Fröhlich for his helpful suggestions during the course of this investigation. I also want to express my thanks to the referee for his valuable suggestions and remarks.

References

[1] S. Adjerid, J.E. Flaherty : *A moving finite element method with error estimation and refinement for one–dimensional time dependent partial differential equations.* SIAM J. Numer. Anal. **23**, pp. 778–796 (1986)

[2] S. Adjerid, J.E. Flaherty : *A local refinement finite element method for two–dimensional parabolic systems* SIAM J. Sci. Stat. Comput. **9**, No. 5, pp. 792–811 (1988)

[3] I. Babuška, A. K. Aziz : *On the angle condition in the finite element method* SIAM J. Num. Anal. **13**, pp. 214–226 (1976)

[4] I. Babuška, W. Rheinboldt *Error estimates for adaptive finite element computations* SIAM J. Numer. Anal. **15**, pp. 736–754 (1978)

[5] R. E. Bank, A. Weiser *Some a posteriori error estimators for elliptic partial differential equations* Math. Comput. **44**, pp. 283–302 (1985)

[6] M. Berzins, P. M. Dew, R. M. Furzeland : *Developing software for time-dependent problems using the method of lines and differential-algebraic integrators.* Appl. Numer. Math. **5**, pp. 375–397 (1989), North-Holland

[7] M. Bieterman, I. Babuška : *The finite element method for parabolic equations. I. A posteriori error estimates* Numer. Math. **40**, pp. 339–371 (1982)

[8] M. Bieterman, I. Babuška : *An adaptive method of lines with error control for parabolic equations of the reaction–diffusion type.* J. Comp. Phys. **63**, pp. 33–66 (1986)

[9] F. A. Bornemann : *An adaptive multilevel approach to parabolic equations I. General theory and 1D–implementation.* IMPACT Comput. Sci. Engrg. **2**, pp. 279–317 (1990)

[10] F. A. Bornemann : *An adaptive multilevel approach to parabolic equations II. Variable-order time discretization based on a multiplicative error correction.* IMPACT Comput. Sci. Engrg. **3**, pp. 93–122 (1991)

[11] F. A. Bornemann : *An adaptive multilevel approach to parabolic equations III. 2D error estimation and multilevel preconditioning.* IMPACT Comput. Sci. Engrg. **4**, pp. 1–45 (1992)

[12] R. Dautray, J.-L. Lions : *Mathematical analysis and numerical methods for science and technology, Vol. 2, Functional and Variational Methods* Springer-Verlag Berlin Heidelberg New York (1988)

[13] L. Demkowicz, J. T. Oden : *On a mesh optimization method based on a minimization of the interpolation error.* Int. J. Engrg. Sci. , Vol. **24**, No. 1, pp. 55–68 (1986)

[14] L. Demkowicz, Ph. Devloo, J. T. Oden : *On a h-type mesh-refinement strategy based on minimization of interpolation errors.* Comp. Meth. Appl. Mech. Engrg. **53**, pp. 67–89 (1985)

[15] P. Deuflhard, P. Leinen, H. Yserentant : *Concepts of an adaptive hierarchical finite element code.* IMPACT Comput. Sci. Engrg. **1**, pp. 3–35 (1989)

[16] P. Deuflhard, E. Hairer, J. Zugck : *One-step and extrapolation methods for differential-algebraic systems.* Numer. Math. **51**, pp. 501–516 (1987)

[17] P. Deuflhard, U. Nowak : *Extrapolation integrators for quasilinear implicit ODEs* In: P. Deuflhard, B. Engquist (eds.): Large Scale Scientific Computing. Progress in Scientific Computing **7**, pp. 37–50 (1987), Birkhäuser

[18] A. R. Diaz, N. Kikuchi, J. E. Taylor : *A method of grid optimization for finite element methods* Comp. Meth. Appl. Mech. Engrg. **41**, pp. 29–45 (1983)

[19] B. Erdmann, J. Lang, R. Roitzsch : *KASKADE – Manual.* Technical Report TR 93–5 (1993), Konrad–Zuse–Zentrum für Informationstechnik Berlin, Germany

[20] K. Eriksson, C. Johnson : *Adaptive streamline diffusion finite element methods for convection–diffusion problems.* Math. Comp., Vol. **60**, No. 201, pp. 167–188 (1993)

[21] E. Hairer, G. Wanner : *Solving ordinary differential equations II, Stiff and differential–algebraic problems.* Springer Series in Comp. Math. **14**, Springer–Verlag

[22] S.A. Iwanow, W.G. Korneew, J. Lang : *Estimates for constants in inequalities of basis elements.* J. Numer. Math. & Math. Phys. **28**, No. 9, Moscow (1988)

[23] P. Jamet : *Estimation d' erreur pour des elements finis droits presque degeneres.* R.A.I.R.O, Serie Analyse Numerique **10**, No. 3, pp. 43–61 (1976)

[24] J. Lang, A. Walter : *A finite element method adaptive in space and time for nonlinear reaction–diffusion systems.* IMPACT Comput. Sci. Engrg. **4**, pp. 269–314 (1992)

[25] J. Lang, A. Walter : *An adaptive Rothe method for nonlinear reaction–diffusion systems.* Appl. Numer. Math. **13**, pp. 135–146 (1993)

[26] J. Lang : *KARDOS – KAskade Reaction Diffusion One–dimensional System.* Technical Report TR 93–9 (1993), Konrad–Zuse–Zentrum für Informationstechnik Berlin, Germany

[27] J. Lawson, M. Berzins, P. M. Dew : *Balancing space and time errors in the method of lines for parabolic equations.* SIAM J. Sci. Stat. Comput., Vol. **12**, No. 3, pp. 573–594 (1991)

[28] R. Lehmann : *Computable error bounds in the finite element method.* IMA J. Numer. Anal. **6**, pp. 265–271 (1986)

[29] A. K. Noor, I. Babuška : *Quality assessment and control of finite element solutions.* Finite Elements Anal. Des. **3**, pp. 1–26 (1987)

[30] U. Nowak : *Adaptive Linienmethoden für nichtlineare parabolische Systeme in einer Raumdimension.* Dissertation, FU Berlin, Fachbereich Mathematik, Technical Report TR 93–14, Konrad–Zuse–Zentrum Berlin (ZIB) (1993)

[31] J. T. Oden, L. Demkowicz : *Advances in adaptive improvements: A survey of adaptive methods in computational fluid mechanics.* In: A. K. Noor and J. T. Oden (eds.): State of the art, Surveys in Computational Mechanics (ASME, New York, 1988)

[32] M. Roche : *Rosenbrock methods for differential algebraic equations.* Numer. Math. **52**, pp. 45–63 (1988)

[33] M. D. Smooke, M. L. Koszykowski *Two–dimensional fully adaptive solutions of solid–solid alloying reactions* J. Comp. Phys. **62**, pp. 1–25 (1986)

[34] J.L. Synge : *The hypercircle in mathematical physics.* Cambridge University Press, New York (1957)